INTERNATIONAL JOURNAL OF MULTIDISCIPLINARY RESEARCH AND ANALYSIS

ISSN(print): 2643-9840, ISSN(online): 2643-9875

Volume 06 Issue 03 March 2023

DOI: 10.47191/ijmra/v6-i3-32, Impact Factor: 7.022

Page No. 1111-1118

Influence of a Magnetic Field on Blood Flow Through an Inclined Tapered Vessel with a Heat Source

K.W. Bunonyo[1], L. Ebiwareme[2]

[1] Department of Mathematics and Statistics, Federal University Otuoke, Nigeria

[2] Department of Mathematics, Rivers State University, Nigeria

ABSTRACT: In this study, we investigated the effect of a heat source on blood flow through a gradient-tapered vessel under the influence of a gradient magnetic field by reformulating the problem using a mathematical model representing the blood momentum and energy equations. The partial differential equations were dimensionlessly scaled using a scaling parameter and further reduced to a system of ordinary differential equations. A coupled system of regular equations was solved using the series method to obtain analytical solutions for temperature and blood velocity profiles. Numerical simulations were performed using Wolfram Mathematica version 12 and varied parameters relevant to the investigation. The results showed that the relevant parameters—magnetic field, radiation parameter, Grashof number, and tilt angle contributed to liquid temperature and blood flow velocity, respectively. The novelty of this study is the fact that heat can be introduced from a heat source for the purpose of helping blood circulation, and magnetic fields tend to accelerate blood flow velocity.

KEYWORDS: Heat source, Blood, Flow, Vessel, Magnetic field, Angle of inclination, Tapered angle

1. INTRODUCTION

Blood flow through blood vessels and atherosclerosis of the cardiovascular system, including hardening of the arteries due to plaque accumulation were studied by solving the underlying equations formulated using several suitable methods. There are several researchers who have investigated blood flow, and they are: Elshehawey and Husseny [1] studied peristaltic transport in ferrofluids with porous boundaries. Sinha and Misra [2] studied blood flow through arteries with permeable walls. Makinde and Osalusi [3] studied steady-state magnetohydrodynamic (MHD) flow in a two-dimensional channel with permeable boundaries. Elangovan and Ratchagar [4] conducted a study of his MHD flow in steady state through a circular vertical pipe with a permeable boundary. Makinde and Chinyoka [5] studied unsteady MHD flow in porous two-dimensional channels with impermeable and porous walls. Sattar and Waheedullah [6] studied the unsteady flow of a viscoelastic fluid through a porous medium surrounded by two porous plates. Xin-Hui Si et al. [7] studied asymmetric laminar flow in porous channels with expanding or contracting walls. A homotopy analysis (HAM) method was employed to obtain the flow profile of the velocity field. Bunonyo and Amos [8] studied blood flow through notched arteries and their results proved useful. Bunyoño et al. [9] formulated a model that studied the blood flow of atherosclerosis and was solved using an analytical approach. Hanvey and Bunonyo [10] discussed the therapeutic effects on blood flow through arteries and showed that increasing the Grashof number resulted in increased blood flow. The problem of unstable aspiration was described by Tsangaris et al. [11]. A case of periodic suction in parallel plate flow was reported by Ramanamurthy et al. [12]. Murthy and Bahali [13] conducted a study of micropolar liquid flow through circular tubes under the influence of a transverse magnetic field with constant suction or injection at the tube wall. Sharma et al. [14] studied the effect of a transverse magnetic field on blood flow in a cylindrical tube containing magnetic particles. Eldesoky [15] studied the slip effect on transient MHD pulsatile blood flow through porous media in arteries under the influence of body acceleration. Similarly, Eldesoky [16] studied the effect of relaxation time on pulsatile MHD blood flow through porous media in arteries under the action of cyclic body acceleration.

The purpose of this article is to extend the work done by Srivastava [17], to investigate the effects of heat and magnetic fields; we reconstructed the problem by introducing the effects of heat sources on blood flow in inclined tapered vessels. , is a thermo-magnetic therapy treatment. Use the series method in solving the governing equations formulated to obtain various flow profiles simulated using Wolfram Mathematica version 12.

2. MATHEMATICAL FORMULATION

According to Srivastava [17], the equation describing the steady flow of blood through the cylindrical artery inclined at an angle α is described as:

$$\rho\vec{F} = -\frac{\partial P^*}{\partial z^*} + \mu\left(\frac{\partial^2 u^*}{\partial r^{*2}} + \frac{1}{r^*}\frac{\partial u^*}{\partial r^*}\right) - \frac{\mu u^*}{k^*} + \vec{J}\times\vec{B} \qquad (1)$$

According to Darcy's law, the blood velocity is:

$$u^* = -\frac{k^*}{\mu}\frac{\partial P^*}{\partial z^*} \qquad (2)$$

Following the current density and magnetic field relation, we have:

$$\vec{J}\times\vec{B} = \sigma\left(\vec{E} + \vec{u}\times\vec{B}\right)\times\vec{B} \qquad (3)$$

$$\beta_T = -\frac{1}{\rho}\left(\frac{\rho - \rho_\infty}{T^* - T_\infty}\right) \qquad (4)$$

Substituting equations (2)-(4) into equation (1), we have the momentum equation reduces to:

$$\rho g sin\alpha = -\frac{\partial P^*}{\partial z^*} + \mu\left(\frac{\partial^2 u^*}{\partial r^{*2}} + \frac{1}{r^*}\frac{\partial u^*}{\partial r^*}\right) + \rho\beta_T\left(T^* - T_\infty\right) - \frac{\mu u^*}{k^*} - \sigma B_0^2 u^* \qquad (5)$$

We shall introduce the energy equation with a source to investigate the effect of heat on equation (5), according to Bunonyo and Amos [8], we have:

$$\rho c_p\frac{\partial T^*}{\partial t^*} = k_T\left(\frac{\partial^2 T^*}{\partial r^{*2}} + \frac{1}{r^*}\frac{\partial T^*}{\partial r^*}\right) + Q_0\left(T^* - T_\infty\right) \qquad (6)$$

Equations (5) and (6) are subject to the following boundary conditions:

$$\left.\begin{array}{ll} u^* = 0, T^* = T_w & \text{at } r^* = h^* \\ \dfrac{\partial u^*}{\partial r^*} = 0, \dfrac{\partial T^*}{\partial r^*} = 0 & \text{at } r^* = 0 \end{array}\right\} \qquad (7)$$

The dimensionless parameters are:

$$\left.\begin{array}{l} z^* = \dfrac{z}{d}, r^* = \dfrac{r}{d_0}, h^* = \dfrac{h}{d_0}, \upsilon^* = \dfrac{b\upsilon}{\delta u}, u^* = \dfrac{u}{u_0}, k^* = \dfrac{k}{d_0^2}, P^* = \dfrac{Pd_0^2}{d\mu\mu_0}, t^* = \dfrac{\upsilon t}{d_0^2}, Rd = \dfrac{Q_0 d_0^2}{\mu c_p} \\ Fr = \dfrac{u_0^2}{gd_0}, M = \dfrac{\sigma d_0^2 B_0^2}{\mu}, Re = \dfrac{\rho u_0 d_0}{\mu}, \theta = \dfrac{T^* - T_\infty}{T_w - T_\infty}, Gr = \dfrac{d_0^2\beta_T\left(T_w - T_\infty\right)}{\upsilon u_0}, Pr = \dfrac{\mu c_p}{k_T} \end{array}\right\} \qquad (8)$$

Following equation (8), equations (5) to (7) are reduced to:

$$\frac{Re}{Fr} sin\alpha = -\frac{\partial P}{\partial z} + \frac{\partial^2 u}{\partial r^2} + \frac{1}{r}\frac{\partial u}{\partial r} - \left(\frac{1}{k} + M^2 cos^2\alpha_1\right)u + \theta Gr \qquad (9)$$

$$Pr\frac{\partial\theta}{\partial t} = \frac{\partial^2\theta}{\partial r^2} + \frac{1}{r}\frac{\partial\theta}{\partial r} + RdPr\theta \qquad (10)$$

The corresponding boundary conditions are:

$$\left.\begin{array}{ll} u = 0, \theta = 1 & \text{at } r = h \\ \dfrac{\partial u}{\partial r} = 0, \dfrac{\partial\theta}{\partial r} = 0 & \text{at } r = 0 \end{array}\right\} \qquad (11)$$

3. REDUCTION TO ORDINARY DIFFERENTIAL EQUATION

Equations (5)-(6) are reduced to system of ordinary differential equations using the following:

$$\left.\begin{aligned} & u = u_0 \\ & \theta = \theta_0 e^{\omega t} \\ & -\frac{\partial P}{\partial z} = P_z \end{aligned}\right\} \tag{12}$$

Using equation (12), equations (9)-(11) are reduced to:

$$\frac{d^2u_0}{dr^2} + \frac{1}{r}\frac{du_0}{dr} - \beta_1^2 u_0 = P_z + \frac{Re}{Fr}Sin\alpha - \theta_0 Gr \tag{13}$$

$$r^2\frac{d^2\theta_0}{dr^2} + r\frac{d\theta_0}{dr} + \beta_2^2 r^2\theta_0 = 0 \tag{14}$$

where $\beta_1^2 = \left(\frac{1}{k} + M^2cos^2\alpha_1\right), \beta_2^2 = \left(Rd - \omega\right)Pr$

The corresponding boundary conditions are:

$$\left.\begin{aligned} & u_0 = 0, \theta_0 = e^{-\omega t} \qquad \text{at } r = h \\ & \frac{du_0}{dr} = 0, \frac{d\theta_0}{dr} = 0 \qquad \text{at } r = 0 \end{aligned}\right\} \tag{15}$$

3.1 Method of Solution

Solving equations (13)-(14), let the solutions be in the following form:

$$\theta_0\left(r\right) = \sum_{n=0}^{\infty} a_n r^{n+\alpha} \tag{16}$$

$$w_0\left(r\right) = \sum_{n=0}^{\infty} a_n r^{n+\alpha} \tag{17}$$

Differentiate equation (16) twice and substitute the results into equation (14), we obtain:

$$\theta_0\left(r\right) = a_0 A J_0\left(\beta_2 r\right) + Ba_0\left[J_0\left(\beta_2 r\right)\log r + \frac{\beta_2^2 r^2}{4}\left(1 - \frac{6\beta_2^2 r^2}{4^3} + \frac{44\beta_2^4 r^4}{4^3.6^3}\right)\right] \tag{18}$$

If $B = 0$, then equation (18) reduces to:

$$\theta_0\left(r\right) = AJ_0\left(\beta_2 r\right) \tag{19}$$

Solving equation (19) using the boundary condition in equation (15), we have:

$$\theta_0\left(r\right) = \frac{e^{-\omega t}J_0\left(\beta_2 r\right)}{J_0\left(\beta_2 h\right)} \tag{20}$$

Substitute equation (20) into equation (13), which is:

$$\frac{d^2u_0}{dr^2} + \frac{1}{r}\frac{du_0}{dr} - \beta_1^2 u_0 = P_z + \frac{Re}{Fr}Sin\alpha - \frac{e^{-\omega t}Gr}{J_0\left(\beta_2 h\right)}J_0\left(\beta_2 r\right) \tag{21}$$

Solving the homogenous part of equation (21), we have:

$$\frac{d^2u_0}{dr^2} + \frac{1}{r}\frac{du_0}{dr} + \left(i\beta_1\right)^2 u_0 = 0 \tag{22}$$

Solving equation (22), we obtained the homogenous solution as:

$$u_{0h}\left(r\right) = AI_0\left(\beta_1 r\right) \tag{23}$$

The particular solution of equation (21) can be presented as:

$$u_{0p} = -\frac{1}{\beta_1^2}\left(P_z + \frac{Re}{Fr}Sin\alpha\right) + \frac{e^{-\omega t}Gr}{\beta_1^2 J_0\left(\beta_2 h\right)}J_0\left(\beta_2 r\right) \tag{24}$$

The solution to equation (21) is the sum of equations (24) and (23), which is:

$$u_0(r) = AI_0(\beta_1 r) - \frac{1}{\beta_1^2}\left(P_z + \frac{Re}{Fr}Sin\alpha\right) + \frac{e^{-\omega t}Gr}{\beta_1^2 J_0(\beta_2 h)}J_0(\beta_2 r) \tag{25}$$

Applying the boundary conditions in equation (15), we can simplify equation (25) as:

$$u_0(r) = \frac{1}{\beta_1^2}\left(P_z + \frac{Re}{Fr}Sin\alpha\right)\left(\frac{I_0(\beta_1 r)}{I_0(\beta_1 h)} - 1\right) + \frac{e^{-\omega t}Gr}{\beta_1^2}\left(\frac{J_0(\beta_2 r)}{J_0(\beta_2 h)} - \frac{I_0(\beta_1 r)}{I_0(\beta_1 h)}\right) \tag{26}$$

Substituting equation (26) into equation (12), we obtained:

$$u(r) = \frac{1}{\beta_1^2}\left(P_z + \frac{Re}{Fr}Sin\alpha\right)\left(\frac{I_0(\beta_1 r)}{I_0(\beta_1 h)} - 1\right) + \frac{e^{-\omega t}Gr}{\beta_1^2}\left(\frac{J_0(\beta_2 r)}{J_0(\beta_2 h)} - \frac{I_0(\beta_1 r)}{I_0(\beta_1 h)}\right) \tag{27}$$

$$\text{where } A = \frac{1}{\beta_1^2 I_0(\beta_1 h)}\left(P_z + \frac{Re}{Fr}Sin\alpha\right) - \frac{e^{-\omega t}Gr}{\beta_1^2 I_0(\beta_1 h)}$$

$$I_0(\beta_1 r) = \left(1 + \frac{\beta_1^2 r^2}{4} + \frac{\beta_1^4 r^4}{64} + \frac{\beta_1^6 r^6}{2304}\right) \text{ and } I_0(\beta_1) = \left(1 + \frac{\beta_1^2}{4} + \frac{\beta_1^4}{64} + \frac{\beta_1^6}{2304}\right)$$

$$J_0(\beta_2 r) = \left(1 - \frac{\beta_2^2 r^2}{2^2} + \frac{\beta_2^4 r^4}{2^2.4^2} - \frac{\beta_2^6 r^6}{2^2.4^2.6^2}\right) \text{ and } J_0(\beta_2) = \left(1 - \frac{\beta_2^2}{2^2} + \frac{\beta_2^4}{2^2.4^2} - \frac{\beta_2^6}{2^2.4^2.6^2}\right)$$

4. RESULTS

This section talks about numerical simulation of the analytical function as solved in the previous section using Mathematica, version 12, where we shall vary the pertinent parameters within a specified range and study the results of the effect of those parameters. The parameters ranges of values we shall consider in the course of the simulation are as follows: $0 \le Pr \le 21, 0 \le Rd \le 10$
$0 \le Re \le 1, 10 \le Gr \le 30, 0 \le M \le 10, 5 \le \alpha \le 25, 0.5 \le h \le 1, 0 \le \alpha_1 \le 1$. The plots below shows the effect of Prandtl number Pr, Reynolds number Re, Grashof number Gc, Magnetic field parameter M, angle of inclination α, tapered angle α_1, the height of stenosis h and radiation parameter Rd on blood temperature $\theta(r,t)$ and blood velocity profile $u(r)$ respectively.

4.1 Effect of Prandtl Number and Radiation Parameter on Blood Temperature

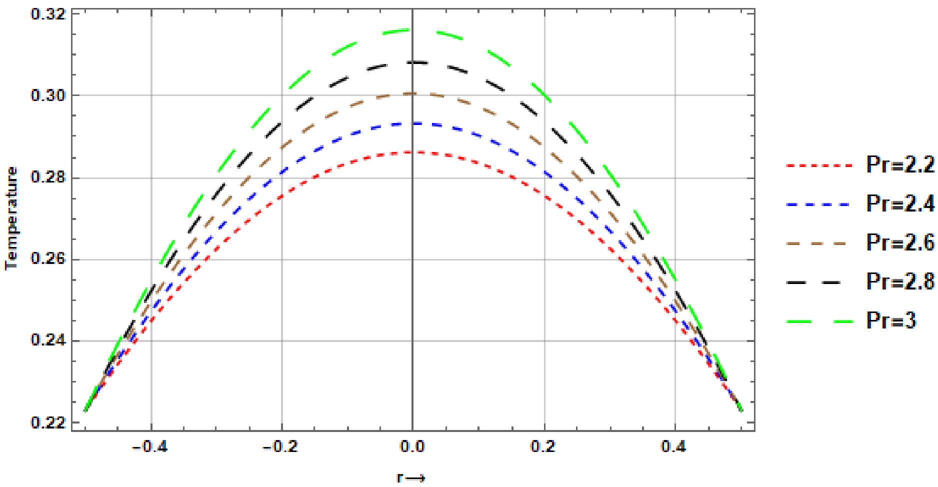

Figure 1. The effect of Prandtl number on Blood Temperature

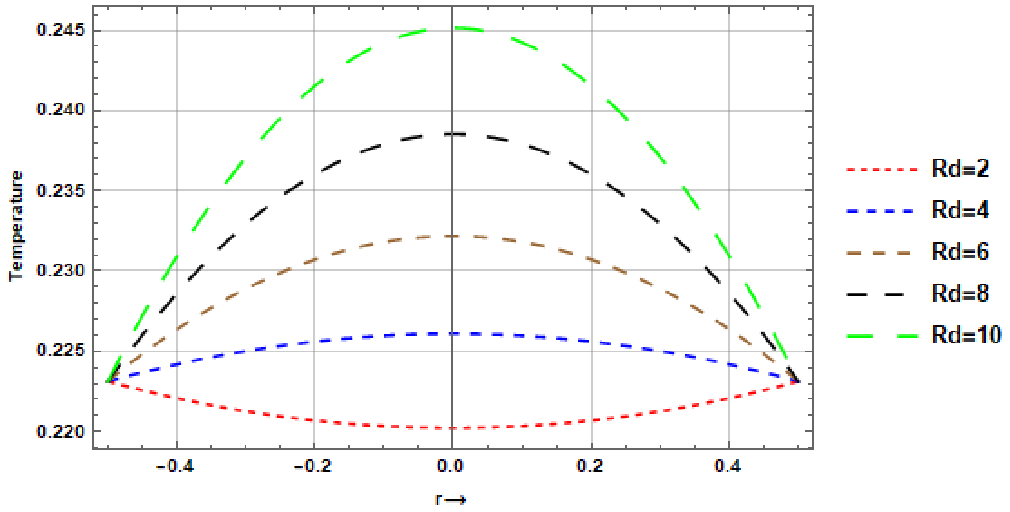

Figure 2. The effect of Heat Source Parameter on Blood Temperature

4.1 Effect of the Different Values of the Pertinent Parameters on Blood Velocity

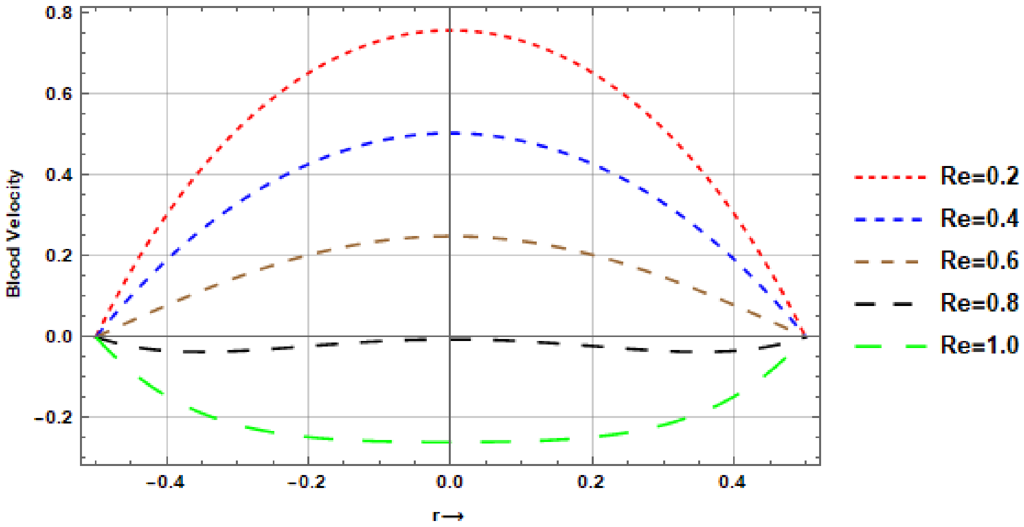

Figure 3. The effect of Reynolds number on Blood Velocity

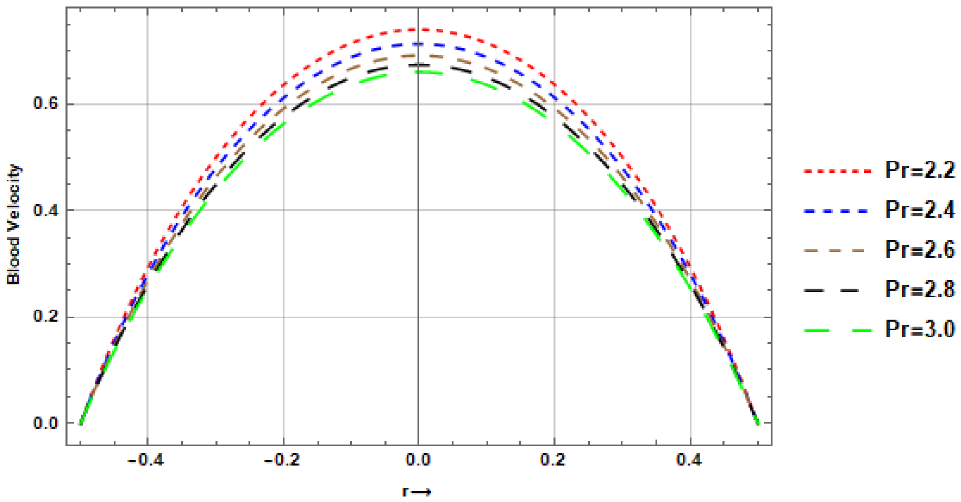

Figure 4. The effect of Prandtl number of Blood Velocity

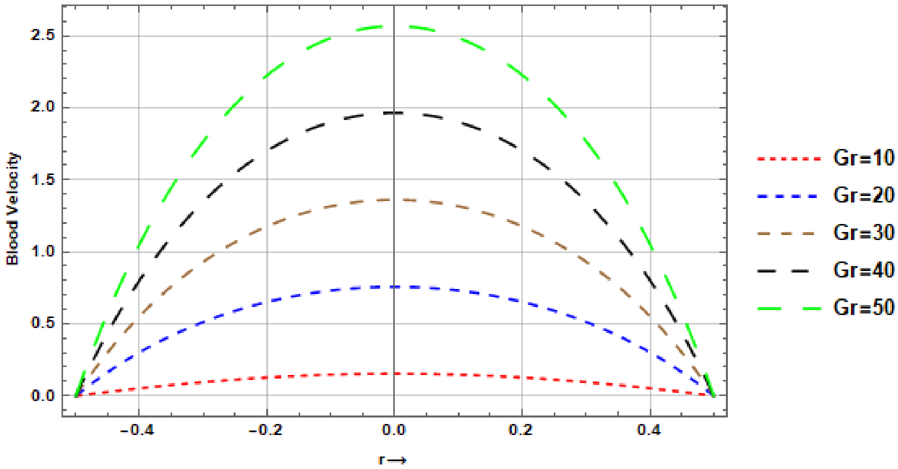

Figure 5. The effect of Grashof number on Blood Velocity

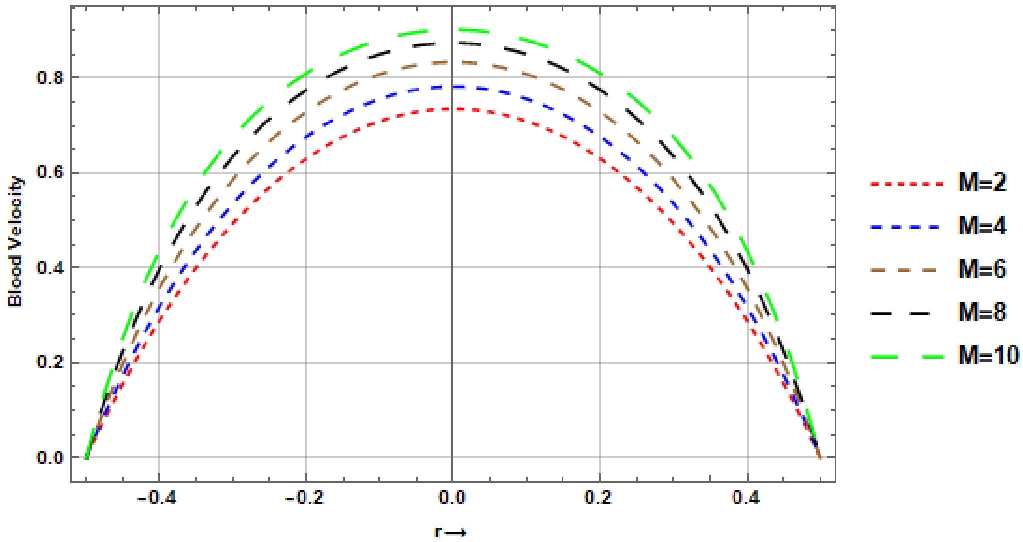

Figure 6. The effect of Magnetic Field on Blood Velocity

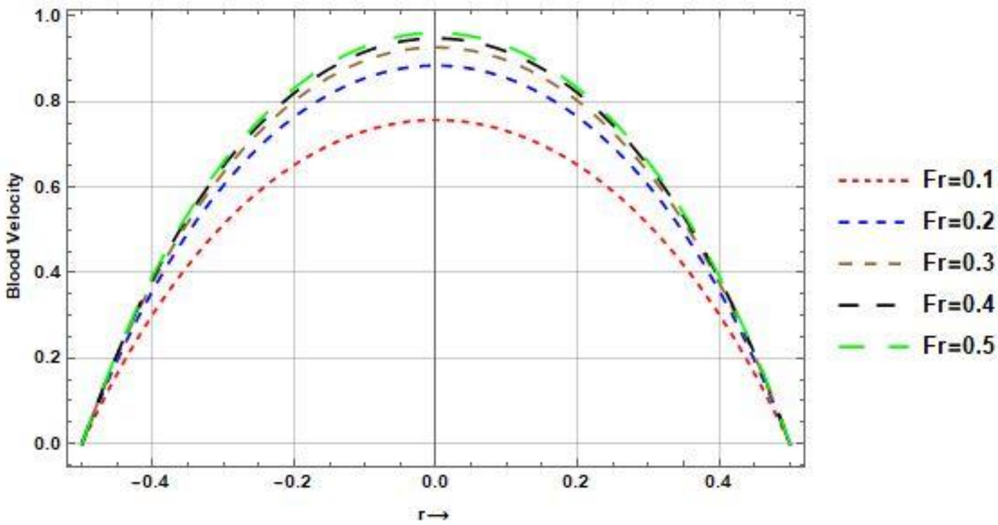

Figure 7. The effect of Froude number on Blood Velocity

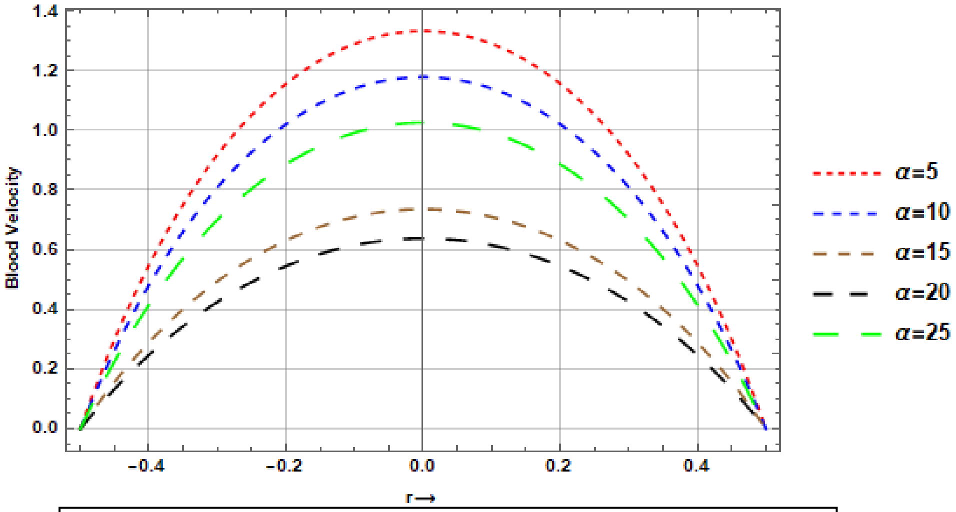

Figure 8. The effect of Angle of Inclination on Blood Velocity

5. DISCUSSION

Mathematical models were formulated to investigate blood flow through a blood vessel at an inclined angle with a tapered angle induced by a magnetic field. The models were scaled and reduced to a system of ordinary differential equations, subject to some specific boundary conditions. In addition, the analytical solutions representing the blood velocity and temperature profiles with some pertinent parameters were simulated using Wolfram Mathematica, version 12, and the results are discussed based on the figures as follows: Figure 1 depicts that the temperature of the fluid increases for an increase in the Prandtl number. This result is consistent with the view that blood temperature can be controlled if the Prandtl number is kept under check. The heat source parameter was investigated, and the result was found to be promising because it is seen in Figure 2 that the temperature of the fluid increases for every increase in heat from the source. This result might be very helpful for patients planning heat therapy.

The Reynolds number effect was also investigated, and the result found in Figure 3 depicts that the blood velocity profile decreases with an increase in Reynolds number. This result is consistent with the view that, for a fixed kinematic viscosity of the fluid in a varying length of the blood vessel, the blood velocity decreases due to the loss of head of the fluid through the vessel. Figure 4 illustrates that the blood velocity decreases with an increase in Prandtl number. It is seen in this figure that the velocity amplitudes are quite close for an increasing Prandtl number of 2.2, 2.4, 2.6, 2.8, and 3.0, respectively.

Figure 5 indicates that the blood velocity increases with an increase in the Grashof number value from 10, 20, 30, 40, and 50 units, respectively. However, every other contributing parameter was made constant, holding its values. If a device with a magnetic field interacts with an electrically conducting fluid, it generates a force called the Lorentz force, which opposes and retards the flow. The effect of magnetic fields on blood flow was investigated, and the results are presented in Figure 6. The figure shows that blood velocity decreases with an increase in magnetic field. The result of this investigation could be very helpful in the detection of tumor growth and treatment.

Figure 7 showed that the Froude number has an effect on blood velocity. The result is based on the view that the blood velocity increases with an increase in Froude number while holding the parameter values of the other parameters constant. This research also investigated the impact of the angle of inclination of blood vessels on blood flow. Figure 8 illustrates that an increase in the angle of inclination of the blood vessel decreases the blood velocity. The results obtained here have made it clear that in solving flow problems, depending on the position or location, the patient positioning should be considered so important as to avoid hypotension.

In conclusion

from our investigation, we have shown that the blood flow through an inclined vessel can be modeled. However, it was seen that the pertinent parameters, such as the magnetic field, radiation parameter, Grashof number, Froude number, and the angle of inclination, all affect the blood temperature and blood circulation, which were not discussed in previous researcher, Srivastava [17].

REFERENCES

1) EF Elshehawey and SZA Husseny. Peristaltic transport of a magneto-fluid with porous bounderies. *Appl. Math. Comput.* 2002; 129, 421-40.
2) Sinha, A., & Misra, J. C. (2012). Influence of Slip Velocity on blood flow through an artery with Permeable Wall: A Theoretical Study. *International Journal of Biomathematics*, *5*(05), 1250042.
3) Makinde, O. D., & Osalusi, E. (2006). MHD steady flow in a channel with slip at the permeable boundaries. *Romanian Journal of Physics*, *51*(3/4), 319.
4) Elangovan, K., & Ratchaga, N. P. (2010). Steady flow through a circular vertical pipe with slip at the permeable boundaries with an applied magnetic field. *Appl. Math. Sci*, *4*, 2445-52.
5) Makinde, O. D., & Chinyoka, T. (2001). Unsteady MHD flow in a porous channel with an exponentially decreasing suction. *J. Pure Appl. Math*, *1*(1), 1-13.
6) Sattar, A., & Waheedullah, A. (2013). Unsteady flow of a visco-elastic fluid through porous medium bounded by two porous plates. *Int. J. Eng. Sci. Tech*, *5*, 329-34.
7) Si, X. H., Zheng, L. C., Zhang, X. X., & Chao, Y. (2011). Homotopy analysis solutions for the asymmetric laminar flow in a porous channel with expanding or contracting walls. *Acta Mechanica Sinica*, *27*(2), 208-214.
8) Bunonyo, K. W., & Amos, E. (2022). Convective Flow of Blood through a Constricted Cylinder and the Effect of Cholesterol Growth Rate on the Motion in the Presence of a Magnetic Field. *African Scientific Reports*, 174-187.
9) Bunonyo, K. W., & Amos, E. (2021). Mathematical Modeling of Mixed LDL-C and Blood Flow through an inclined Channel with Heat in the presence of Magnetic Field. In *9th (Online) International Conference on Applied Analysis and Mathematical Modeling (ICAAMM21) June 11-13, 2021, Istanbul-Turkey* (p. 143).
10) Hanvey, R. R., & Bunonyo, K. W. (2022). Effect of Treatment Parameter on Oscillatory Flow of Blood Through an Atherosclerotic Artery with Heat Transfer. *Journal of the Nigerian Society of Physical Sciences*, 682-682.
11) Tsangaris, S., Kondaxakis, D., & Vlachakis, N. W. (2007). Exact solution for flow in a porous pipe with unsteady wall suction and/or injection. *Communications in Nonlinear Science and Numerical Simulation*, *12*(7), 1181-1189.
12) Ramanmurthy, J. V., Srinivasacharyulu, N., & Odelu, O. (2007). Viscous fluid flow between two parallel plates with periodic suction and injection. *AMSE J. Model. B: Mech. Thermic*, *50*, 29-37.
13) Murthy, J. R., Bahali, N. K., & Srinivasacharya, D. (2010). Unsteady flow of micropolar fluid through a circular pipe under a transverse magnetic field with suction/injection. *Selçuk Journal of Applied Mathematics*, *11*(2), 13-25.
14) Sharma, G. C., Jain, M., & Singh, A. (2009). Mathematical Analysis of MHD Flow of Blood in Very Narrow Capillaries (RESEARCH NOTE). *International Journal of Engineering*, *22*(3), 307-315.
15) Eldesoky, I. M. (2012). Slip effects on the unsteady MHD pulsatile blood flow through porous medium in an artery under the effect of body acceleration. *International Journal of Mathematics and Mathematical Sciences*, *2012*.
16) Eldesoky, I. M. (2013). Effect of relaxation time on MHD pulsatile flow of blood through porous medium in an artery under the effect of periodic body acceleration. *Journal of Biological Systems*, *21*(02), 1350011.
17) Srivastava, N. (2014). Analysis of flow characteristics of the blood flowing through an inclined tapered porous artery with mild stenosis under the influence of an inclined magnetic field. *Journal of Biophysics*, *1-10*.